GaMnAs for Mid-Wave Infrared Photodetection

Yan-Feng Lao, A. G. Unil Perera, *Fellow, IEEE*, H. L. Wang, and J. H. Zhao

Abstract—The use of GaMnAs as the emitter of an internal-photoemission (IPE) photodetector is studied. As a result of significantly high concentration of holes, GaMnAs-based IPE detector resembles a Schottky-barrier detector, which has the higher absorption and thus enhanced spectral response by comparing with the previously reported *p*-type GaAs/AlGaAs detectors. A GaMnAs/AlGaAs detector is expected to fully cover the $3-5$-μm range of detection. The theoretical value of the responsibility is 0.0133 A/W at 3.5 μm.

Index Terms—Infrared photodetector, GaAs, III-V, semiconductor, valence band.

I. INTRODUCTION

THE *p*-type optical transitions involving the valence bands (VBs) [1] have shown potential applications in internal photoemission (IPE) heterojunction photodetectors [2]. In particular, $1 - 10$ μm heterojunction detectors were demonstrated [3], [4] by making use of the inter-valence-band (IVB) transitions. Furthermore, the hole transition from the heavy-hole (HH) band to the spin-orbit split-off (SO) band has been used to demonstrate the $3-5$ μm detection without the need of cooling [3], [4]. IPE detectors based on the heterojunction structures are subject to limitations: 1) the absorption characteristics of the emitter (which is responsible for photon absorption) mostly affected by the electronic structure; for example, an absorption dip around 3.6 μm observed in *p*-type GaAs/AlGaAs detectors resulting from the inter-valence-band transitions; and 2) lower absorption coefficient of doped semiconductors compared to that of the metal which was initially used as the emitter in Schottky barrier detectors [5]. The absorption characteristics of *p*-type GaAs are greatly influenced by its split-off gap between the HH and SO bands. The energy of the split-off gap (0.339 eV [6]) is the onset of the SO-HH transition, corresponding to the forbidden SO-HH transition at the Γ point. For this reason, there is a dip in the absorption around 3.6 μm and therefore, *p*-type GaAs/AlGaAs heterojunction detectors display a similar response dip as reported in the past studies [3], [4]. Such a dip is undesired for a $3-5$ μm detection.
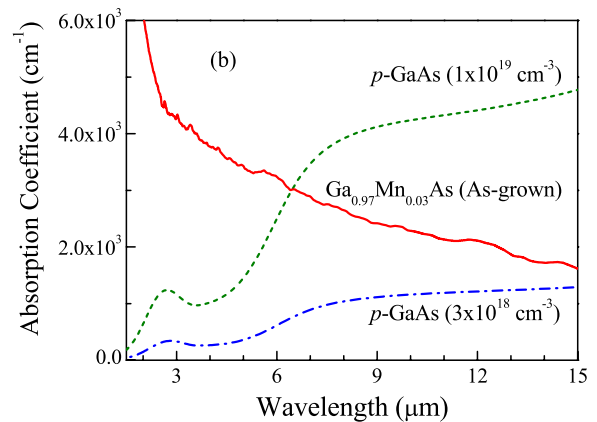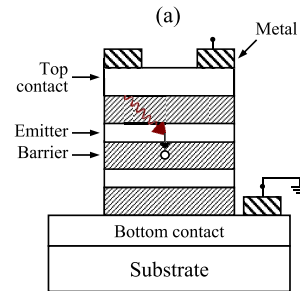
Fig. 1. (a) Schematic of a multiple periodic GaMnAs/AlGaAs IPE detector. (b) Comparison of the absorption coefficient of GaMnAs with that of *p*-type GaAs. The absorption of GaMnAs was obtained from the dielectric function by applying a model-independent fitting algorithm to experimental reflection and transmission spectra [8], and the absorption of *p*-type GaAs was calculated based on a model dielectric function [1]. The inset shows a similar comparison by excluding the intra-band free-carrier absorption.

In this letter, we discuss the use of a dilute magnetic semiconductor (GaMnAs) to develop a room-temperature $3-5$ μm IPE detector, as schematically shown in Fig. 1 (a). GaMnAs is a *p*-type semiconductor and contains free holes. Its hole concentration is significantly higher (up to 10^{21} cm^{-3}) than regular *p*-type semiconductors doped with non-magnetic dopant such as Be (up to 10^{19} cm^{-3}) and Carbon (up to 10^{20} cm^{-3}). It is thus possible to have an even higher absorption over *p*-type GaAs by using GaMnAs. Furthermore, with the increase in the hole concentration and the shift of the Fermi level downward deep into the VBs, as well as the increase of the plasma frequency, [1] the absorption peak shifts towards the short wavelength and becomes broadened due to enhanced carrier scatterings [7]. As a consequence, the absorption dip at Δ_0 can be removed, which leads a GaMnAs based IPE detector to fully cover the $3-5$ μm range of detection.

II. THEORETICAL MODEL

GaMnAs is demonstrated to be promising in achieving higher absorption owing to its very high concentration of

holes compared to p-type GaAs and continuum absorption ranging from 3 to 5 μm, [8] as shown in Fig. 1 (b). The p-type absorption originates mainly from the HH-to-SO and HH-to-light hole (LH) transitions, which have the corresponding wavelength ranges of $1-4$ μm and $4-15$ μm, respectively. In contrast to the typical free-carrier absorption characteristic by the intra-band transitions in p-type GaAs which increases with wavelength, [1] absorption of $Ga_{0.97}Mn_{0.03}As$ decreases with increasing wavelength, and is much greater than that of p-type GaAs between $3-5$ μm. This characteristic can be related to the very high concentration of holes in GaMnAs. For example, a concentration of 5×10^{19} cm^{-3}–5×10^{20} cm^{-3} is expected in samples with a Mn fraction of 0.03 [9]. With a higher hole concentration, the Fermi level moves downward, leading to the LH-HH transitions taking place at large values of the wave vectors. Reference [8] showed that the absorption peak moves from around 8.5 μm at $p = 10^{17}$ cm^{-3} to 5.5 μm at $p = 10^{20}$ cm^{-3} for GaAs [4]. Furthermore, the plasma frequency also increases at the higher hole concentration. All of these reasons, along with enhanced carrier scatterings leading to absorption broadening, [7] contribute to the removal of the absorption dip at Δ_0. This also leads a featureless absorption, as shown in Fig. 1 (b). These characteristics make GaMnAs to be suitable for mid-wave infrared (MWIR) detectors.

As shown in Fig. 1 (a), the IPE detector consists of an active region which is sandwiched between two p-type doped (top and bottom) contact layers. The active region comprises multiple periodic units of a p-type emitter (absorber) and an undoped AlGaAs barrier. The potential barrier height at the emitter-barrier interface determines the dark current and response threshold.

The computation of the spectral response is based on an escape cone model [10] which is used to evaluate the emission probability of the IPE process. The idea is to calculate the number of carriers which are capable of escaping over a potential barrier by having a normal (to the interface) momentum greater than that of the barrier. These carriers occupy energy states on a spherical Fermi cap in k space [11]. This model can extract the threshold energy of photoemission, [11], [12] and simulate the spectral response of heterojunction photodetectors in terms of free-carrier absorption [10], [13]. To calculate the spectral response, the total quantum efficiency is calculated, including the escape efficiency (probability), and the absorption efficiency. The latter takes into account absorption of the emitter, i.e., intra- and inter-valence-band optical transitions. The responsivity is then calculated by [13]

$$R = \eta g_p \frac{q}{hc} \lambda \tag{1}$$

where η is the total quantum efficiency, g_p is the gain, q is the electron charge and λ is the wavelength. η can be obtained as $\eta = \eta_i \eta_a$, where η_a is the absorption efficiency, and η_i is the photoemission efficiency. The other symbols have their usual meaning. The absorption efficiency is obtained by using the following equation,

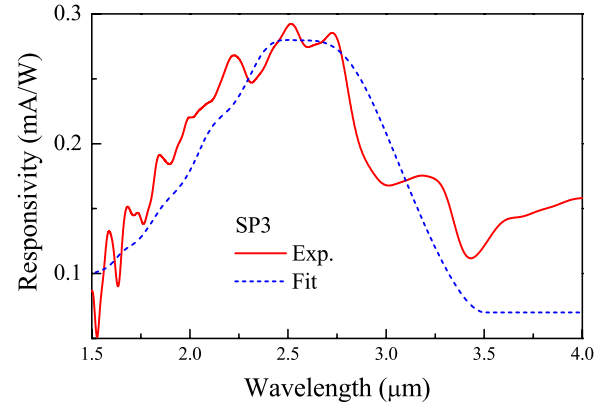$$\eta_a = 2 \frac{\omega}{c} \text{Im}[\epsilon(\omega)] \frac{1}{E_0^2} \int_0^W E(z)^2 dz \tag{2}$$

Fig. 2. Comparison of experimental response and simulation for p-type GaAs with $p = 3 \times 10^{18}$ cm^{-3}, where the dashed line is calculated based on an escape cone model. The experimental response is take from [3].

where $\text{Im}[\epsilon(\omega)]$ is the imaginary part of the dielectric function, ω is the frequency, E is the electric field of the light inside the layer, E_0 is the electric field of the incident light, and W is the thickness of the emitter.

III. RESULTS AND DISCUSSION

The spectral response is calculated based on a periodic structure which consists of 30 periods of a 20 nm-thick emitter and a 60 nm-thick $Al_xGa_{1-x}As$ barrier. The Al fraction of the barrier is varied in order to achieve specific response threshold and over the detection range of $3-5$ μm. The response is firstly simulated in order to fit the response of the previously reported split-off detector operating at room temperature (sample SP3) [3]. As shown in Fig. 2, the overall fitting agrees with the experimental response well, while the deviation at about 3 μm is due to indirect transitions which are not considered in the present calculation. The response calculated here uses the absorption data extracted from experimental reflection and transmission spectra based on a model-independent fitting algorithm [8]. The distinct difference between the detection in a device and the absorption in a material is that the absorbed photons contribute electrical currents only when photoexcited carriers are being able to escape over the potential barrier. The escape process typically involves transfer of carriers between the emitter and barrier. Holes can be optically excited in the emitter by either direct or indirect transitions. For the near-threshold regime, holes must end up at states near the potential barrier in order to escape; [14] in this case, indirect transitions could lead to a higher probability of transfer and thus an enhanced response.

In terms of the simulated response, we carried out computations of response for detectors that use GaMnAs as the emitter. Fig. 3 plots the absorption efficiency. The multiple peaks overlapped on the curves are due to the interference modes in the multiple-layer structure. As shown in the experimental response (Fig. 2), they are nearly equidistant in energy between adjacent peaks, which is a characteristic of the optical interference. Two GaMnAs samples have been used in this study in order to compare the response between different Mn fractions. As the hole concentration is proportional to the Mn fraction, a sample with the higher Mn fraction will
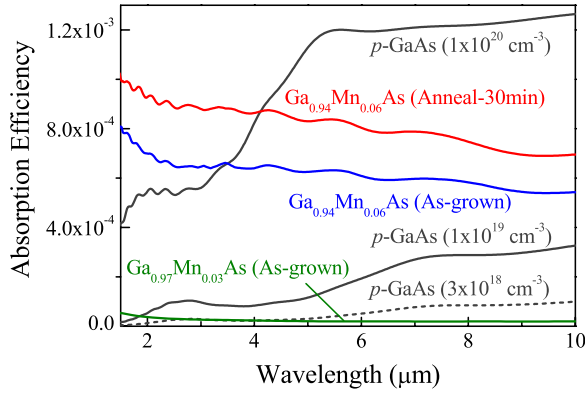
Fig. 3. The calculated absorption efficiency for the heterojunction detector structures which includes *p*-type GaAs and GaMnAs emitters. The absorption dip around 3.6 μm in *p*-type GaAs reduces the absorption efficiency by comparing with the structure using GaMnAs as the emitter.
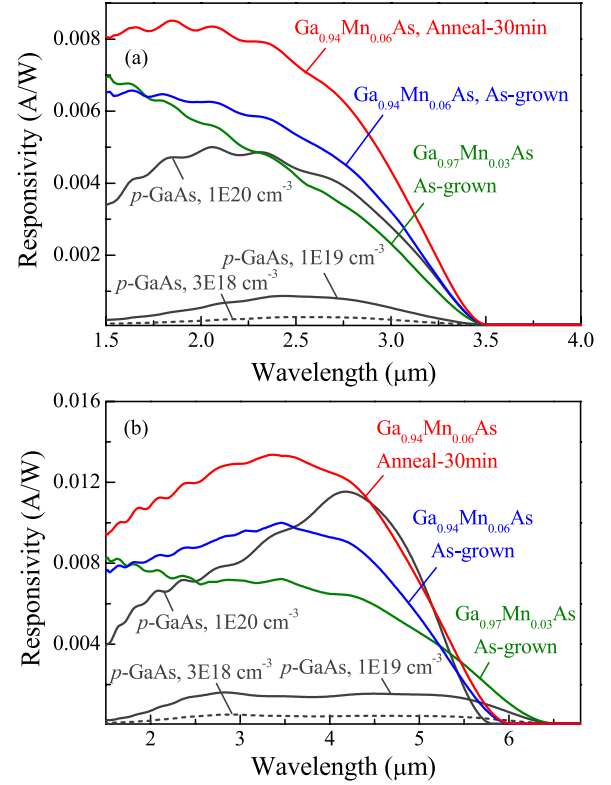

Fig. 4. Comparison of calculated response of the detector structures using different emitters. The computation is carried out for (a) the same response thresholds and (b) different response thresholds (in order to cover the $3-5$ μm wavelength range). The response dip is distinct in the *p*-type GaAs structures with doping concentrations of 3×10^{18} cm^{-3} and 1×10^{19} cm^{-3}.

correspondingly own a higher absorption. The Mn dopants can partially stay in the interstitial positions. It is thus a necessary step to carry out post-growth annealing process to increase the hole concentration. The absorption of the annealed samples is then obtain using the model-independent fitting algorithm (for details see [8]).

Based on the obtained absorption coefficient, the absorption efficiency is calculated as shown in Fig. 3. Annealing at 230 °C with a duration of 30 minutes leads to an increase in the absorption efficiency. The general spectral profile remains the same although a significantly higher absorption is attained by using either a higher Mn fraction or annealing. The decrease in the absorption efficiency at long wavelengths is a consequence of the reduced the intra-band free carrier absorption in the long-wavelength range. In contrast, the intra-band free carrier absorption is significant in regular *p*-type doped GaAs, and actually dominates when the hole concentration increases to a higher level, for example, at $p = 1 \times 10^{20}$ cm^{-3}. By comparing with the absorption efficiency in the $3-5$ μm range, the 1×10^{20} cm^{-3} *p*-type doped GaAs is lower than that of Ga$_{0.94}$Mn$_{0.06}$As, which is due in part to the absorption dip at around 3.6 μm.

To compare the performance between devices using regular *p*-type GaAs and GaMnAs as the emitter, we set the IPE threshold the same as sample SP3 [3] (*p*-type GaAs with $p = 3 \times 10^{18}$ cm^{-3}). Fig. 4 (a) shows the calculated results. The response of Ga$_{0.97}$Mn$_{0.03}$As/AlGaAs detector has about 8 times improvement over that of SP3. With an increase in the hole concentration of *p*-type GaAs, the response increases as well; however, the Ga$_{0.94}$Mn$_{0.06}$As/AlGaAs detector still has the higher response than the *p*-type GaAs detector even with a doping concentration of $p = 1 \times 10^{20}$ cm^{-3}. This result is due to the absence of absorption dip at around 3.6 μm in GaMnAs. To achieve the $3-5$ μm of detection, the threshold wavelengths of each detector structures are individually adjusted (via varying the potential barriers, i.e., Al fraction of the AlGaAs layer). Calculated results are shown in Fig. 4 (b). The enhancement factor of response for the GaMnAs detector compared to the regular *p*-type GaAs is similar to the results shown in Fig. 4 (a). However, the *p*-type GaAs detectors

display response dip at about 3.6 μm; with a higher doping concentration of $p = 1 \times 10^{20}$ cm^{-3}, such a dip is indistinct, due to much enhanced free carrier absorption. The response of the GaAs detector with $p = 1 \times 10^{20}$ cm^{-3} is mainly contributed by the free-carrier absorption, while the GaMnAs detector operates in terms of the inter-valence-band transitions. The GaMnAs detector demonstrates better response compared to $p = 1 \times 10^{20}$ cm^{-3} doped GaAs detector. The growth of GaMnAs requires a much lower temperature than that of the regular GaAs-based devices, which raises a concern of the material quality; however, low-temperature grown GaAs has been already used to fabricate devices, such as the terahertz emitters [15]. It is thus feasible to use low-temperature grown GaMnAs to fabricate IPE detector devices.

IV. CONCLUSION

To conclude, the response of GaMnAs/Al$_x$Ga$_{1-x}$As heterojunction detectors compared to regular *p*-type GaAs/Al$_x$Ga$_{1-x}$As detector is reported. The results indicate that the GaMnAs/Al$_x$Ga$_{1-x}$As detector shows a full coverage of response over the $3-5$ μm range, while the regular *p*-type GaAs/Al$_x$Ga$_{1-x}$As detector has a response dip around 3.6 μm. By comparing with the previously demonstrated sample SP3, the use of Ga$_{0.97}$Mn$_{0.03}$As as the absorber will gain 8 times improvement in response. In addition, GaMnAs has a much high absorption and thus will be suitable for the photodetector working in the MWIR range.

REFERENCES

[1] Y.-F. Lao and A. G. U. Perera, "Dielectric function model for *p*-type semiconductor inter-valence band transitions," *J. Appl. Phys.*, vol. 109, no. 10, p. 103528, 2011.

[2] F. D. Shepherd, Jr., V. E. Vickers, and A. C. Yang, "Schottky barrier photodiode with a degenerate semiconductor active region," U.S. Patent 3 603 847, Sep. 7, 1971.

[3] P. V. V. Jayaweera, S. G. Matsik, A. G. U. Perera, H. C. Liu, M. Buchanan, and Z. R. Wasilewski, "Uncooled infrared detectors for 3–5 μm and beyond," *Appl. Phys. Lett.*, vol. 93, no. 2, p. 021105, 2008.

[4] Y. F. Lao *et al.*, "Light-hole and heavy-hole transitions for high-temperature long-wavelength infrared detection," *Appl. Phys. Lett.*, vol. 97, no. 9, p. 091104, 2010.

[5] A. Rogalski and M. Kimata, *Infrared Photon Detectors* (SPIE Press Monographs). Bellingham, WA, USA: SPIE, 1995.

[6] Y.-F. Lao, A. G. U. Perera, L. H. Li, S. P. Khanna, E. H. Linfield, and H. C. Liu, "Direct observation of spin-orbit splitting and phonon-assisted optical transitions in the valence band by internal photoemission spectroscopy," *Phys. Rev. B*, vol. 88, p. 201302, Nov. 2013.

[7] R. Newman and W. W. Tyler, "Effect of impurities on free-hole infrared absorption in *p*-type germanium," *Phys. Rev.*, vol. 105, no. 3, pp. 885–886, Feb. 1957.

[8] Y. F. Lao, A. G. U. Perera, H. L. Wang, J. H. Zhao, Y. J. Jin, and D. H. Zhang, "Optical characteristics of *p*-type GaAs-based semiconductors towards applications in photoemission infrared detectors," *J. Appl. Phys.*, vol. 119, no. 10, p. 105304, 2016.

[9] M. J. Seong, S. H. Chun, H. M. Cheong, N. Samarth, and A. Mascarenhas, "Spectroscopic determination of hole density in the ferromagnetic semiconductor $Ga_{1-x}Mn_xAs$," *Phys. Rev. B*, vol. 66, no. 3, p. 033202, Jul. 2002.

[10] M. B. Rinzan, S. Matsik, and A. G. U. Perera, "Quantum mechanical effects in internal photoemission THz detectors," *Infr. Phys. Technol.*, vol. 50, nos. 2–3, pp. 199–205, Apr. 2007.

[11] R. Williams, *Injection Phenomena* (Semiconductors and Semimetals), R. Willardson and A. Beer, Eds. New York, NY, USA: Academic, 1970.

[12] A. M. Goodman, "Photoemission of electrons from *n*-type degenerate silicon into silicon dioxide," *Phys. Rev.*, vol. 152, no. 2, pp. 785–787, Dec. 1966.

[13] D. G. Esaev, M. B. M. Rinzan, S. G. Matsik, and A. G. U. Perera, "Design and optimization of GaAs/AlGaAs heterojunction infrared detectors," *J. Appl. Phys.*, vol. 96, no. 8, pp. 4588–4597, 2004.

[14] Y.-F. Lao and A. G. U. Perera, "Temperature-dependent internal photoemission probe for band parameters," *Phys. Rev. B*, vol. 86, p. 195315, Nov. 2012.

[15] M. Awad, M. Nagel, H. Kurz, J. Herfort, and K. Ploog, "Characterization of low temperature GaAs antenna array terahertz emitters," *Appl. Phys. Lett.*, vol. 91, no. 18, p. 181124, 2007.